Journal of Nuclear Materials 386–388 (2009) 479–482

Contents lists available at ScienceDirect

Journal of Nuclear Materials

journal homepage: www.elsevier.com/locate/jnucmat

Effects of aluminum on high-temperature strength of 9Cr–ODS steel

S. Ohtsuka *, T. Kaito, M. Inoue, T. Asayama, S.W. Kim, S. Ukai [1], T. Narita [2], H. Sakasegawa [3]

Advanced Nuclear System R&D Directorate, Japan Atomic Energy Agency, 4002 Narita, Oarai, Ibaraki 311-1393, Japan

ABSTRACT

This paper discusses the effects of small amount of Al contamination (<0.1 wt%) on high-temperature strength and microstructure of the 9Cr–ODS steel. Increasing Al concentration degraded the ultimate tensile strength as well as the 0.2% proof stress at 973 K and 1073 K accompanied by decreasing fraction of the elongated grain, i.e., residual-α ferrite acting as reinforcement phase. The decrease of residual-α ferrite proportion provided by increasing Al is contrary to general behavior of conventional steels. Computer simulation on ferrite to austenite phase transformation suggested that the fine oxide dispersion in the elongated ferrite could be attributable to the preferential partitioning of Ti and W in ferrite than in austenite at hot-extrusion process.

1. Introduction

Oxide dispersion strengthened (ODS) ferritic/martensitic steel containing 9 wt%Cr (9Cr–ODS steel) is a promising material that has the potential to keep microstructural stability and satisfactory mechanical properties even under the high-dose neutron irradiation brought to fusion reactor blanket materials as well as fast reactor fuel cladding materials. Aluminum addition is known to appreciably coarsen the dispersed oxide particles and deteriorate high-temperature strength of ODS steels [1], while Al is often used as deoxidization material in steel production so that a small amount of Al could be contaminated into raw material powders. Moreover, the contamination from a ball mill container may take place in the course of mechanical alloying (MA). This paper discusses the effects of small amount of Al contamination on the high-temperature strength and microstructure of 9Cr–ODS steel.

2. Experimental procedure

The 9Cr–ODS steel round bars containing 0.03–0.085 wt% Al were produced with a general process consisting of MA and subsequent hot-extrusion at 1423 K as described in a report [2], where the standard composition of JAEA 9Cr–ODS steel for fast reactor application, i.e., Fe–9wt%Cr–2W–0.2Ti–0.35Y_2O_3, was chosen for basic chemical composition except for Al contents. Chemical analysis results of the steel bars are shown in Table 1, where specimen ID AL0XY means the steel containing 0.0XY wt% Al, e.g. AL017 contains 0.017 wt%Al. Argon-gas atomized ferritic powders slightly containing Al were used for AL017, and elemental powders (Fe, Cr, C, W, Ti, Al) for the rest of steels together with yttria (Y_2O_3) powders. Uni-axial tensile tests were performed for normalized-and-tempered steels (1323 K × 1 h, Ar-gas cooling => 1073 K × 1 h, Ar-gas cooling) at temperatures of 973 K and 1073 K with the load parallel to extrusion direction. The field-emission type transmission electron microscope (FE-TEM) and optical microscope were used for microstructure characterizations. Vickers microhardness measurements were performed to grasp matrix microhardness distribution.

3. Results and discussion

3.1. Tensile properties

Fig. 1 shows the tensile test results of the normalized-and-tempered steels. At each test temperature, increasing Al reduces the ultimate tensile strength, while the slope of 0.2% proof stress curve is fairly small. The degradation of ultimate tensile strength with small yield strength deterioration appears to be a typical behavior of dual-phase alloy strengthened by reinforcement phase [3]. In the dual-phase alloy, plastic deformation is considered to start and localize in low strength matrix. This localized plastic deformation should provide higher work hardening rate producing higher ultimate tensile strength than the deformation in the single phase material without reinforcement phase.

3.2. Microstructures

Fig. 2 presents the TEM views, where specimens were fully annealed with the condition of the 1323 K × 1 h annealing followed by the furnace-cooling at 30 K/h, because the presence of high

* Corresponding author.
E-mail address: ohtsuka.satoshi@jaea.go.jp (S. Ohtsuka).
[1] Present address: Hokkaido University, Sapporo 060-8628, Japan.
[2] Present address: Mitsubishi Materials Corporation, Okegawa, Saitama 363-8510, Japan.
[3] Present address: Saclay Center, CEA, 91191 Gif-sur-Yvette cedex, France.

0022-3115/$ - see front matter © 2008 Elsevier B.V. All rights reserved.
doi:10.1016/j.jnucmat.2008.12.147

Table 1
Chemical analysis (wt%) and Vickers hardness test results (Hv).

ID	AL017	AL024	AL050	AL085
C	0.13	0.14	0.14	0.14
Cr	9.0	9.0	8.9	8.9
W	2.0	1.9	2.0	2.0
Ti	0.20	0.20	0.20	0.20
Al	*0.017*	*0.024*	*0.050*	*0.085*
Y	0.29	0.28	0.28	0.28
O	0.14	0.16	0.16	0.16
Y_2O_3 [a]	0.37	0.36	0.36	0.36
Ex.O [b]	0.062	0.084	0.084	0.084
HV [c]	383	382	379	346
H_v(F) [d]	425	430	408	–
SE [e]	3.3	5.9	2.1	–
Hv(M) [f]	348	352	347	340
SE	7.6	2.0	1.0	1.0

[a] Estimated from yttrium content with the assumption that yttrium exists as Y_2O_3.
[b] Defined as the value obtained by subtracting oxygen conc. in Y_2O_3 from the total oxygen conc. in steel.
[c] Vickers hardness (Hv).
[d] Average microhardness of elongated grain (Hv).
[e] Standard error of average microhardness.
[f] Average microhardness of equiaxed grain (Hv).

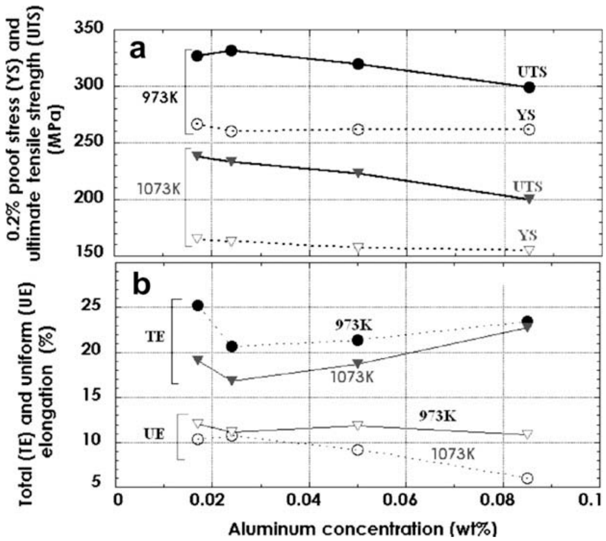

Fig. 1. High temperature tensile properties, (a) 0.2% proof stress (YS) and ultimate tensile strength (UTS), (b) total (TE) and uniform elongation(UE).

density dislocations in the normalized-and-tempered condition brings about considerable difficulty in precise observation of nano-sized oxide particles. As seen in Fig. 2(a) and (b) displaying low magnification TEM views, interconnected small grains having high dislocation density (area fraction (S_f) = 20%) are present in AL050 (0.50 wt%Al), while only coarse equiaxed grains in AL085 (0.085 wt%Al). These interconnected small grains are observed in AL017, AL024 and AL050 (Al $\leqslant$ 0.050 wt%), in which elongated grains are observed by optical microscope. In the full annealing heat treatment, austenite grains are newly produced by ferrite to austenite transformation at the 1323 K annealing, and then transform to annealed coarse ferrite grains by subsequent furnace-cooling whose cooling rate is smaller than the minimal cooling rate permitting the martensite transformation. On the other hand, residual-α ferrite retained at the 1323 K annealing do not undergo any phase transformations, thus keeping relatively high density dislocations pinned by dispersed oxide particles that are present even at 1323 K, while in the conventional heat-resistant steels, dislocations in δ-ferrite are annealed because of the dissolution of MX particles at 1323 K. Therefore, interconnected small grains containing relatively high dislocation density are supposed to be residual-α ferrite that remained untransformed into austenite (γ) even at the 1323 K annealing. Our studies showed that the formation of this residual-α ferrite appreciably improves the tensile and creep strength of 9Cr–ODS steel [4]. Cayron et al reported the similar microstructures in full annealed ODS EUROFER containing Y_2O_3, and came to a conclusion based on dilatometric measurement study of phase transformation that the interconnected small grains are ferrite grains untransformed into austenite (γ) at high-temperature consolidation process [5], and that proportion of untransformed ferrite in martensite is a most important factor for strength improvement. In the 9Cr–ODS steel investigated in this study, addition of Al appears to decrease the proportion of residual-α ferrite phase, which is contrary to the general behavior in conventional steels. The detailed mechanism is unknown, but this unique behavior could be peculiar to the mechanically-alloyed alloys whose microstructures are in non-equilibrium state. Fig. 2(c) and (d) show typical high-magnification TEM views in the coarse equiaxed grain and the interconnected small grain of AL050, which indicate that the latter tends to contain higher population of fine oxide particles than the former. It is reported that nano-sized oxide particles do not coarsen even by aging at 1423 K up to 243 h [6], so that oxide particle observation in these fully annealed specimens should agree with the observation of the normalized-and-tempered specimens. Average oxide particle radius of each 9Cr–ODS steel was evaluated by image analysis of TEM micrographs, and the results are indicated in Table 2, which shows that increasing Al concentration up to 0.085 wt% produces little change in particles size. The extraction replica/EDS analysis results of dispersed oxide particles are also presented in Table 2, which indicates that the dispersed oxide particles are Y–Al–Ti complex oxide, and that Ti in the oxide particle is replaced by Al with increasing Al concentration. This is ascribed to lower standard enthalpy of formation for alumina than titania, which permits oxygen to preferentially combine with Al rather than Ti. It is noteworthy that in AL050 (0.050 wt%Al), oxide particles contain only limited amount of Ti, however their size are kept adequately fine (2.6 nm radius in average in residual-α ferrite). Kasada et al. reported a dispersion of coarsened Y–Al complex oxide particles (3.7 nm radius in average) that does not contain Ti in the 19Cr–4.6Al–ODS ferritic steel (19 wt%Cr–4.6Al–0.3Ti–0.37Y_2O_3) based on STEM/EDS analysis [1]. The Y–Al oxide particles in the 19Cr–4.6Al–ODS is surely larger than those in the residual-α ferrite matrix of AL050. The limited amount of Ti in the oxide particle of AL050 may retard the particle coarsening.

Vickers microhardness measurements were carried out at 49 measurement points for the normalized-and-tempered specimens. The measured points were arrayed in a square lattice (seven rows of seven points) with a separation distance of 25 μm. The size of indent was ~5 μm. Microhardness was roughly Hv400–430 on elongated grains and Hv320–360 on equiaxed grains. This result is consistent with the TEM observations displaying higher population of oxide particles in the interconnected small grains relevant to elongated grain than in the equiaxed grain. The dual-phase specimens (AL017, AL024 and AL050) containing elongated grain therefore have a microstructure similar to composite material containing reinforcement phase, while the single phase specimen (AL085) has a uniform microstructure without reinforcement. Therefore, it is supposed that the decreasing fraction of this reinforcement phase deteriorates the tensile strength with increasing Al concentration.

Yttria powders and matrix metal powders decompose into its constituent elements and dissolve in matrix during MA process

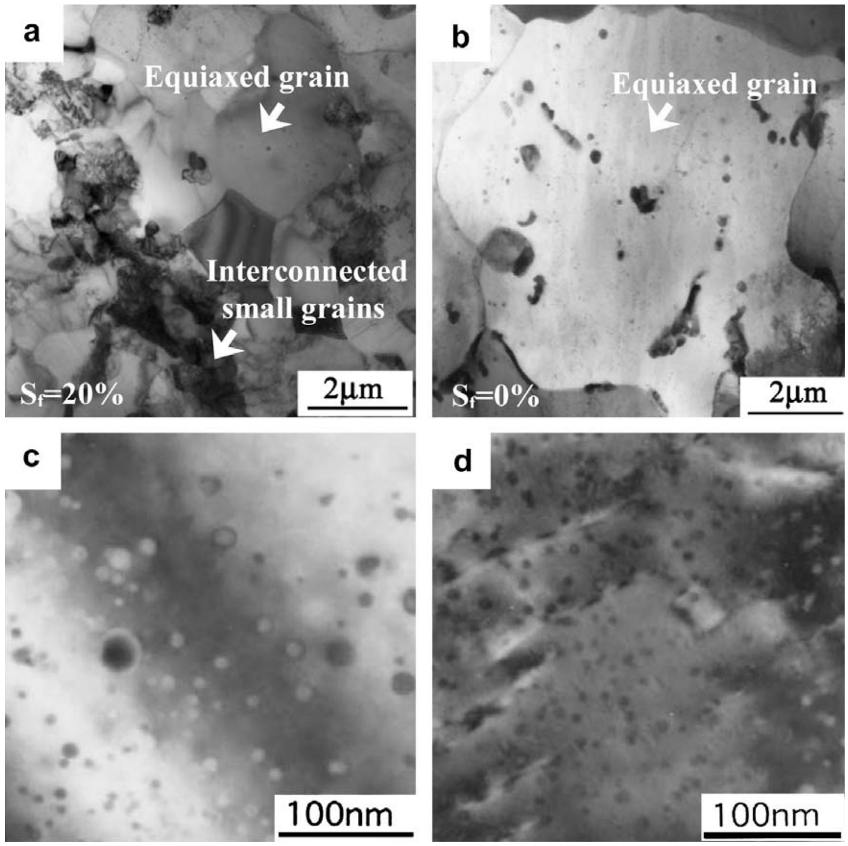

Fig. 2. Transmission electron microscope (TEM) views, typical low magnification views of (a) AL050 (0.050 wt%Al) and (b) AL085 (0.085 wt%Al), and typical intra-grain views in (c) the coarse equi-axed grain and (d) the interconnected small grain of AL050 (0.050 wt% Al).

Table 2
The image analysis results of oxide particle size and the extraction replica/EDS analysis results of the particle composition.

ID	Al (wt%)	In elongated grain			In equi-axed grain			Composition (at.%)		
		R (nm)[a]	SE[b]	N[c]	R (nm)	SE	N	Al	Ti	Y
AL024	0.024	2.6	0.03	742	4.0	0.07	519	11	32	57
AL050	0.050	2.6	0.02	1043	3.9	0.14	341	22	13	65
AL085	0.085	(No elongated grain)			4.7	0.16	255	28	8	64

[a] Average radius of oxide particle (nm).
[b] Standard error of average radius.
[c] Number of particles measured.

[7]. In the subsequent hot-extrusion, nano-sized oxide particles precipitate in the matrix [7]. Matrix chemical composition at hot-extrusion process could have a notable impact on the precipitation. In the course of pre-heating in hot-extrusion process, the matrix undergoes the ferrite to austenite reverse phase transformation, in which solute elements keep on diffusing and being partitioned into each phase. Indeed, the authors revealed an apparent partitioning of W and Cr into the elongated residual-α ferrite in a dual-phase 9Cr–ODS steel powder after 1423 K annealing followed by water-quenching [4]. In order to discuss the effect of solute partitioning on particle precipitation, kinetics of the ferrite to austenite phase transformation was simulated using the software DICTRA with TC-FE3 thermodynamic database and PFRIB kinetic database [8], where the validity of these databases has been verified for multi-component steels. The chemical composition Fe–9wt %Cr–0.13C–2W–0.2Ti–0.050Al and a temperature T = 1423 K were chosen for the simulation. One dimensional simulation was performed with the geometry that single austenite phase nucleates and grows in the 20 μm length ferrite matrix. Fig. 3 presents the simulation results, in which chemical equilibrium calculation results using Thermo-calc and TC-FE3 database are indicated (solid line). It is noted that considerable amount of W and Ti are partitioned into ferrite in the course of the transformation as well as in the equilibrium state. Ferrite forming elements such as W, Ti, Cr and Al are preferentially partitioned into ferrite in the process forcing the chemical potential of each solute element in ferrite to balance with that in austenite. The equilibrium calculation results indicate that Cr and W concentrations in ferrite are, respectively 1.1 and 1.6 times as large as those in austenite. This result is roughly consistent with the semi-quantitative EPMA mapping result of 9Cr–ODS powder after 1423 K × 1 h annealing followed by water-quenching [4]. It was reported that increase of Ti concentration [2] as well as addition of W [9] surely permit the increase of oxide particle population accompanied by particle size reduction in ODS ferritic steels. The partitioning of Ti and W into ferrite at 1423 K hot-extrusion process therefore would be a key factor for

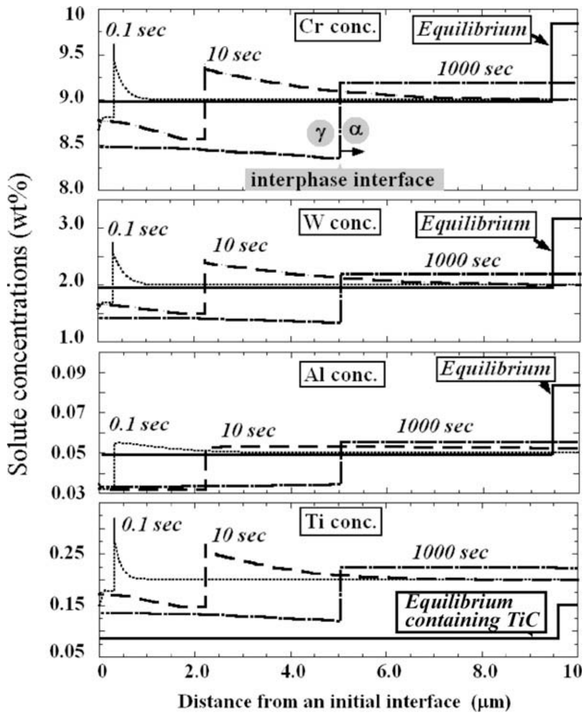

Fig. 3. Computer simulation results on ferrite to austenite reverse transformation using the software DICTRA with TC-FE3 and PFRIB data base [9].

high population particle dispersion in residual-α ferrite than in martensite. It is noted that Al is also partitioned into ferrite. However, the absolute value is in quite a low level since total amount of Al is small, so that the effects of W and Ti partitioning would predominate in the precipitation behavior rather than Al partitioning.

4. Summary

The results of this study are summarized as follows:

(1) Increasing Al concentration in the level lower than 0.1 wt% provides small reduction of ultimate tensile strength and 0.2% proof stress at 973 K and 1073 K.
(2) Degradation of tensile strength is ascribed to the decreasing proportion of elongated grains acting as reinforcement phase in the 9Cr–ODS steel.
(3) Higher population of oxide particle dispersion in the elongated ferrite could be attributable to the preferential partitioning of Ti and W in ferrite than in austenite in the hot-extrusion process.

Acknowledgement

The authors are pleased to thank Dr. M. Fujiwara and Mr. T. Nakai, Kobelco research institute, for valuable discussions throughout the work.

References

[1] R. Kasada, T. Toda, H.S. Cho, A. Kimura, Proceedings of ICAPP'05, May 15–19, 2005, paper 5328.
[2] S. Ukai, T. Okuda, M. Fujiwara, T. Kobayashi, S. Mizuta, H. Nakashima, J. Nucl. Sci. Technol. 39 (2002) 782.
[3] Yo Tomota, Imao Tamura, Tetsu-to-hagane 67 (3) (1981) 439.
[4] S. Ohtsuka, S. Ukai, M. Fujiwara, T. Kaito, T. Narita, Mater. Trans 46 (3) (2005) 487.
[5] C. Cayron, E. Rath, I. Chu, S. Launois, J. Nucl. Mater. 335 (2004) 83.
[6] M.J. Alinger, G.R. Odette, D.T. Hoelzer, J. Nucl. Mater. 329–333 (2004) 382.
[7] T. Okuda, M. Fujiwara, J. Mater. Sci. Lett. 14 (1995) 1600.
[8] J.-O. Andersson, T. Helander, L. Hoglund, P. Shi, B. Sundmann, Calphad 26 (2) (2002) 273.
[9] I.S. Kim, B.Y. Choi, C.Y. Kang, T. Okuda, P.J. Maziasz, K. Miyahara, ISIJ Int. 43 (2003) 1640.